Contribution from the Department of Chemistry, North Carolina State University, Raleigh, North Carolina 27695-8204, and Laboratoire de Chimie Theorique, Université de Paris-Sud, 91405 Orsay Cedex, France

Charge Density Wave as a Probable Cause for the Phase Transition at 125 K in the Ternary Molybdenum Oxide $La_2Mo_2O_7$

Myung-Hwan Whangbo*[†] and Enric Canadell*[‡]

Received October 2, 1986

Tight-binding band calculations were performed to investigate the electronic structure of $La_2Mo_2O_7$. Our calculations reveal that $La_2Mo_2O_7$ is a pseudo-one-dimensional metal, and the two partially filled d-block bands it has lead to Fermi surface nesting with the wave vectors $\mathbf{q}_1 \simeq (0.5a^*, 0.73c^*)$ and $\mathbf{q}_2 \simeq (0, 0.27c^*)$. The charge density waves (CDW) associated with these nesting vectors are expected to cause the phase transition of $La_2Mo_2O_7$, which occurs around 125 K. Furthermore, the bottom of an empty band lies above but very close to the Fermi level in $La_2Mo_2O_7$, so that the CDW's are expected to exhibit an interesting temperature dependence.

Recently, McCarroll et al.[1] prepared single crystals of $La_2Mo_2O_7$ by fused-salt electrolysis of a mixture of Na_2MoO_4, MoO_3, and La_2O_3. Other ternary oxides of molybdenum $R_2Mo_2O_7$ (R = Y, Sm-Lu) obtained by solid-state reactions[2-4] are polycrystalline and magnetically insulating.[5] In contrast, $La_2Mo_2O_7$ is metallic down to 125 K, below which it undergoes a phase transition.[6] This phase transition is also detected by magnetic susceptibility measurements.[6] $La_2Mo_2O_7$ has a pseudo-two-dimensional (2D) crystal structure[6] as does the molybdenum blue bronze $A_{0.3}MoO_3$ (A = K, Rb),[7] which exhibits a charge density wave (CDW).[8] Thus, it was suggested[6] that the phase transition in $La_2Mo_2O_7$ is associated with a CDW. In the present work, we carry out out tight-binding band electronic structure calculations[9] on $La_2Mo_2O_7$ based upon the extended Hückel method[10] in order to probe the nature of its phase transition. The atomic parameters employed in our calculations were taken from ref 8e.

Crystal Structure

It is convenient to describe the crystal structure of $La_2Mo_2O_7$ in terms of its building blocks, MoO_6 octahedra. **1a** is a perspective

1a

1b

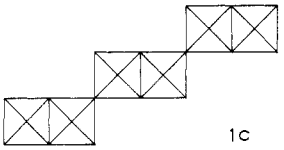

1c

view of an Mo_2O_{10} cluster that is obtained when two MoO_6 octahedra share an edge. Such Mo_2O_{10} clusters form a chain of composition Mo_2O_8 by sharing their "axial" oxygen atoms. The projection view of this chain along the chain axis (i.e., the crystallographic c axis of $La_2Mo_2O_7$) is represented by **1b**. Then, as shown in **1c**, the Mo_2O_8 chains form an Mo_2O_7 slab by sharing their diagonally positioned "equatorial" oxygen atoms. The $La_2Mo_2O_7$ crystal consists of such Mo_2O_7 slabs, which are separated by layers of La^{3+} cations.

According to the formal oxidation of $(La^{3+})_2(Mo_2O_7^{6-})$, each Mo_2O_7 slab carries the formal charge of -6 per Mo_2O_7 formula so that each molybdenum is in the oxidation state Mo^{4+} (d^2). In each Mo_2O_{10} cluster of $La_2Mo_2O_7$, the Mo-Mo distance across the shared edge is 2.478 Å, which is compatible with the Mo-Mo distance that contains a double bond between Mo atoms.[11] The bottom six d-block orbitals of an Mo_2O_{10} cluster are derived primarily from the t_{2g} levels of each metal ion. They are σ_+ (**2a**), σ_- (**2b**), π_+ (**3a**), π_- (**3b**), δ_+ (**4a**), and δ_- (**4b**), where the subscripts + and - indicate that the d orbitals are combined in phase and out of phase, respectively. It is noted that only the metal d orbitals are shown in **2-4** for simplicity.

2a 2b

3a 3b

4a 4b

Band Electronic Structure

The bottom six d-block bands calculated for a 2D $Mo_2O_7^{6-}$ slab are shown in Figure 1. These bands are largely represented by the bottom six d-block orbitals of each Mo_2O_{10} cluster shown in **2-4**. Along the chain direction $\Gamma \rightarrow Y$, the σ bands (σ_+ and σ_-) are flat whereas the π bands (π_+ and π_-) have a substantial dispersion as do the δ bands (δ_1 and δ_2). This is expected because both the π and δ orbitals (**3** and **4**, respectively) make strong π-type overlaps with the p orbitals of the shared "axial" oxygen atoms along the chain direction while the σ orbitals (**2**) do not overlap with any orbitals of the shared "axial" oxygen. The π and δ bands are much less dispersive along the interchain direction $\Gamma \rightarrow X$ than along the chain direction $\Gamma \rightarrow Y$, but the opposite is the case with the σ bands.

[†] North Carolina State University.
[‡] Université de Paris-Sud.

(1) McCarroll, W. H.; Darling, C.; Jakubicki, G. *J. Solid State Chem.* **1983**, *48*, 189.
(2) McCarthy, G. J. *Mater. Res. Bull.* **1971**, *6*, 31.
(3) Hubert, P. H. *Bull. Soc. Chim. Fr.* **1974**, 2385; **1975**, 475, 2643.
(4) Hubert, P. H. *C. R. Seances Acad. Sci., Ser. C* **1977**, *285*, 567.
(5) Subramanian, M. A.; Avavamudan, G.; Subba Rao, G. B. *Mater. Res. Bull.* **1980**, *15*, 1401.
(6) Moini, A.; Subramanian, M. A.; Clearfield, A.; DiSalvo, F. J.; McCarroll, W. H., in press.
(7) (a) Graham, J.; Wadsley, A. D. *Acta Crystallogr.* **1966**, *20*, 93. (b) Ghedira, M.; Chenavas, J.; Marezio, M.; Marcus, J. *J. Solid State Chem.* **1985**, *57*, 300.
(8) (a) Schlenker, C.; Dumas, J. In *Crystal Chemistry and Properties of Materials with Quasi-One-Dimensional Structures*; Rouxel, J., Ed.; Reidel: Dordrecht, The Netherlands, 1986; p 135. (b) Pouget, J. P.; Noguera, C.; Moudden, A. H.; Moret, T. *J. Phys. (Les Ulis, Fr.)* **1985**, *46*, 1731. (c) Fleming, R. M.; Schneemeyer, L. F.; Moncton, D. E. *Phys. Rev. B: Condens. Matter* **1985**, *31*, 899. (d) Sato, M.; Fujishita, H.; Hoshino, S. *J. Phys. C* **1985**, *18*, 2603. (e) Whangbo, M.-H.; Schneemeyer, L. F. *Inorg. Chem.* **1986**, *25*, 2424.
(9) Whangbo, M.-H.; Hoffmann, R. *J. Am. Chem. Soc.* **1978**, *100*, 6093.
(10) Hoffmann, R. *J. Chem. Phys.* **1963**, *39*, 1397.
(11) (a) Chisholm, M. H.; Kelly, R. L.; Cotton, F. A.; Extine, M. W. *J. Am. Chem. Soc.* **1978**, *100*, 2256. (b) Chisholm, M. H.; Cotton, F. A.; Extine, M. W.; Kelly, R. L. *Ibid.* **1979**, *101*, 7645. (c) Cotton, F. A.; Walton, R. A. *Multiple Bonds between Metal Atoms*; Wiley: New York, 1982; p 287.

0020-1669/87/1326-0842$01.50/0

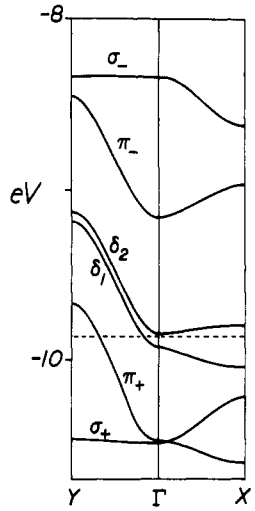

Figure 1. Six low-lying d-block bands for a 2D $Mo_2O_7^{6-}$ slab, where Γ, X, and Y are the wave vector points (0, 0), ($a^*/2$, 0), and (0, $c^*/2$), respectively, in the first Brillouin zone of the reciprocal space. The dahsed line refers to the Fermi level.

In each Mo_2O_{10} cluster, the σ_+, σ_-, π_+, and π_- bands have the metal character of the σ_+, σ_-, π_+, and π_- orbitals, respectively. The δ_1 and δ_2 bands have the metal character of the δ_+ and δ_- orbitals, respectively, along Γ→Y. Along Γ→X, however, the metal orbital character of the δ_1 and δ_2 bands switches so that the δ_1 and δ_2 bands at X have the metal character of the δ_- and δ_+ orbitals, respectively. This switch of the orbital character is caused by the p orbitals of the shared "equatorial" oxygen atoms, whose participation in bonding depends upon the wave vector.[8b,12] The δ_1 and δ_2 bands at Γ have the orbital characters of **5a** and **5b**, respectively, but those at X have the orbital characters of **6a**

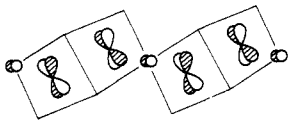

5b

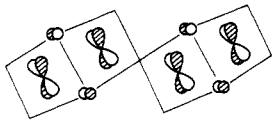

5a

and **6b**, respectively. When the oxygen p orbitals are allowed by

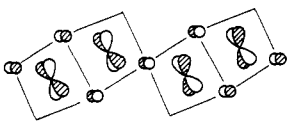

6b

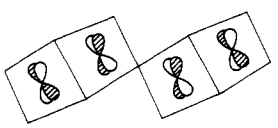

6a

symmetry to interact with the metal d orbitals, the former make an antibonding contribution to the d-block levels, thereby raising their energies. With four d electrons to fill the d-block bands of

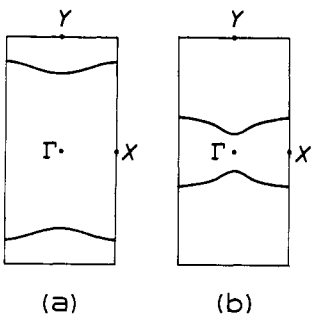

Figure 2. Fermi surface associated with (a) the π_+ band and (b) the δ_1 band. In each case, the region of the wave vectors enclosed by the Fermi surface including Γ leads to filled band levels and the other region leads to unfilled band levels.

Figure 1, the σ_+ band is completely filled and the π_+ and δ_1 bands are partially filled. The σ_+ and π_+ bands have metal–metal-bonding character across the shared edge in each Mo_2O_{10} cluster. On the other hand, the filled portion of the δ_1 band has mostly metal-metal antibonding character. This antibonding effect of the δ_1 band is expected to cancel some of the bonding effects of the σ_+ and π_+ bands. Nevertheless, the Mo–Mo distance of 2.487 Å in $La_2Mo_2O_7$ is extremely short, due presumably to the fact that the antibonding effect of the δ_1 band is negligible by virtue of its weak δ-type overlap between metal ions.

Fermi Surface and CDW

The Fermi surface of a partially filled metallic band is defined as the boundary surface of wave vectors that separate the wave vectors leading to filled band levels from those leading to unfilled band levels. Shown in parts a and b of Figure 2 are the Fermi surfaces associated with the bands π_+ and δ_1, respectively. In either part a or part b of Figure 2, the Fermi surface consists of two separate pieces, which are curved. Thus, $La_2Mo_2O_7$ is a pseudo-one-dimensional (1D) metal with the best electrical conductivity along the chain direction Γ→Y (i.e., the crystallographic c direction).

One piece of a Fermi surface may be superimposable, by translating it with a wave vector **q**, onto another piece of the Fermi surface. In such a case, the two pieces are said to be nested by the vector **q**. A metallic system with a nesting vector **q** gives rise to a CDW of wave vector **q**, which can be detected by diffuse X-ray scattering as diffuse reflections in between the meain Bragg reflections.[13]

For the Fermi surface of the π_+ band shown in Figure 2a, the lower piece is nested to the upper one by the wave vector $\mathbf{q}_1 \simeq (0.5a^*, 0.73c^*)$. The Fermi surface of the δ_1 band shown in Figure 2b has a greater curvature near Γ than near X, so that the lower and the upper pieces are not well nested. Nevertheless, away from the region of Γ, the upper piece of the π_+-band Fermi surface is similar in curvature to that of the δ_1-band Fermi surface. Thus, the former is nested, though incompletely near the region of Γ, to the latter by the wave vector $\mathbf{q}_2 \simeq (0, 0.27c^*)$. Likewise, the lower piece of the π_+-band Fermi surface is approximately nested to that of the δ_1-band Fermi surface by $\mathbf{q}_2$. Such a nesting does not remove all the Fermi surface after the corresponding CDW is formed, which therefore would leave some metallic character even after the CDW formation.[14]

According to the above discussion, it is likely that $La_2Mo_2O_7$ has CDW's of wave vectors $\mathbf{q}_1 \simeq (0.5a^*, 0.73c^*)$ and $\mathbf{q}_2 \simeq (0, 0.27c^*)$, and such CDW's are responsible for the phase transition in $La_2Mo_2O_7$. Another important feature of the band structure of Figure 1 is that the bottom of the δ_2 band lies above but very close to the Fermi level (0.018 eV above). Therefore, as in the

(12) Whangbo, M.-H. In *Crystal Chemistry and Properties of Materials with Quasi-One-Dimensional Structures*; Rouxel, J., Ed.; Reidel: Dordrecht, The Netherlands, 1986; p 27.

(13) Moret, R.; Pouget, J. P. In *Crystal Chemistry and Properties of Materials with Quasi-One-Dimensional Structures*; Rouxel, J., Ed.; Reidel: Dordrecht, The Netherlands, 1986; p 87.

(14) Monceau, P. In *Electronic Properties of Inorganic Quasi-One-Dimensional Compounds*; Monceau, P., Ed.; Reidel: Dordrecht, The Netherlands, 1985; p 139.

case of the molybdenum blue bronze $A_{0.3}MoO_3$ (A = K, Rb),[8b,e] thermal excitation of electrons can occur from the π_+ and δ_1 bands into the bottom portion of the δ_2 band. This thermal excitation, which increases with temperature, shrinks the occupied region of wave vectors in both part a and and part b of Figure 2. As a consequence, the two pieces of the Fermi surface of either the π_+ and the δ_1 band come closer to each other upon losing electrons by thermal excitation. Then, the c^* component of $\mathbf{q}_1$ would decrease from $0.73c^*$ upon increasing temperature, whereas that of $\mathbf{q}_2$ would remain nearly temperature-independent.

Concluding Remarks

The present band electronic structure calculations on an $Mo_2O_7^{6-}$ slab show that $La_2Mo_2O_7$ is a pseudo-1D metal, with the strongest electric conductivity along the crystallographic c direction, and has two partially filled bands. These bands give rise to two nesting vectors $\mathbf{q}_1 \simeq (0.5a^*, 0.73c^*)$ and $\mathbf{q}_2 \simeq (0, 0.27c^*)$. Thus the CDW's associated with these nesting vectors are likely to be responsible for the phase transition in $La_2Mo_2O_7$, which occurs around 125 K. As in the case of the molybdenum blue bronze $A_{0.3}MoO_3$ (A = K, Rb), $La_2Mo_2O_7$ has the bottom of an empty band lying above but very close to the Fermi level. Thus, to fully understand the nature of the phase transition in $La_2Mo_2O_7$, it would be important not only to search for the presence of CDW's but also to probe their temperature dependence.

Acknowledgment. M.-H.W. thanks Prof. W. H. McCarroll and A. Moini for discussion and a copy of a preprint of their work prior to publication. This work is in part supported by the Office of Basic Sciences, Division of Materials Science, DOE, under Grant DE-FG05-ER45259, and also by NATO, Scientific Affairs Division.

Registry No. $La_2Mo_2O_7$, 12142-72-2.

Contribution from the Anorganisch-Chemisches Institut der Universität Heidelberg, 6900 Heidelberg, FRG

Synthesis, Antitumor Activity, and X-ray Structure of Bis(imidazolium) (Imidazole)pentachlororuthenate(III), $(ImH)_2(RuImCl_5)$

B. K. Keppler,* D. Wehe, H. Endres, and W. Rupp

Received July 1, 1986

The X-ray structure, an improved synthesis, and the antitumor activity of $(ImH)_2(RuImCl_5)$ are described. $(ImH)_2(RuImCl_5)$, $(C_3H_5N_2)_2[RuCl_5(C_3H_4N_2)]$, $M_r = 484.59$, is orthorhombic, space group C_{2v}^{12}-$Bm2_1b$, with $a = 8.464$ (2) Å, $b = 14.406$ (3) Å, $c = 14.936$ (4) Å, $V = 1821$ Å^3, $Z = 4$, $D_{calcd} = 1.77$ g cm^{-3}, and final $R_w = 0.038$, for 764 reflections and 75 variables. The antitumor activity was investigated in the P 388 leukemia model. The lifespan of the animals treated with $(ImH)_2(RuImCl_5)$ was increased up to T/C values of 150–162%. This effect was in the same range as that observed with the positive controls 5-fluorouracil and cisplatin. These clinically used drugs increased the lifespan in the same experiment up to T/C values of 144% and 175%, respectively.

Introduction

During the last 20 years, since *cis*-diamminedichloroplatinum(II) (INN: cisplatin) was discovered as a potent tumor-inhibiting agent that, in clinical studies, turned out to be a drug with its best activity against testicular cancer, much more work has been done in the field of antitumor-active metal complexes than before this date.[1] Most of the efforts were concentrated on platinum as the central metal. Thousands of platinum complexes were synthesized for this reason, and more than 1000 were investigated in preclinical tests for antitumor activity. But the clinical trials with a number of new platinum compounds, selected by way of these methods for the first treatment of patients, demonstrated clearly the relatively close pharmacological and toxicological behavior of the new derivatives compared with the original cisplatin. The spectrum of tumors the derivatives exhibited activity against was not broader than that of cisplatin, and myelosuppression was the dose-limiting side effect, as in the case of cisplatin, also. A small amount of success was achieved with a few derivatives concerning the nephrotoxicity and neurotoxicity.[2-6]

Owing to these facts, it is necessary to search for non-platinum complexes, which may exhibit tumor-inhibiting properties against other tumors than the established antitumor agents and which may prove to have less severe side effects. We recently discovered the tumor-inhibiting bis(β-diketonato)metal complexes. One of these compounds, diethoxybis(1-phenylbutane-1,3-dionato)titanium(IV) (INN: budotitane), has reached clinical phase 1 studies now.[7]

Interesting work in the field of antitumor-active ruthenium complexes has been done previously.[8] In this paper we will present bis(imidazolium) (imidazole)pentachlororuthenate(III), $(ImH)_2(RuImCl_5)$, as a representative of a new class of water-soluble, heterocycle-coordinated ruthenium complexes with anticancer activity.

The antitumor activity of $ImH(RuIm_2Cl_4)$, another compound of this class, was described by us recently.[9]

Table I. Crystallographic and Experimental Details

cryst shape; size, mm	prism; 0.08 × 0.1 × 0.15
cryst syst	orthorhombic
space group	$Bm2_1b$ (C_{2v}^{12}, No. 36)
a, b, c, Å	8.464 (2), 14.406 (3), 14.936 (4)
λ, Å	0.7107
μ, cm^{-1}	15.9
min transmission (max = 1)	0.87
max 2θ, deg	60
range of hkl	000 to 7,19,20
possible observns	1328
observns used in refinement ($I > 2.5\sigma(I)$)	764

(1) Sigel, H. *Met. Ions Biol. Syst.* **1980**, *11*.
(2) Zwelling, L. A. *EORTC Cancer Chemotherapy Annual*; Pinedo, H. M., Chapner, B. A., Eds.; Elsevier: Amsterdam, 1985; Vol. 7, pp 105–122.
(3) Vermorken, J. B.; ten Bokkel Huinink, W. W.; McVie, J. G.; van der Vijgh, W. J. F.; Pinedo, H. M. *Dev. Oncol.* **1984**, *17*, 330–343.
(4) Sternberg, C.; Cheng, E.; Sordillo, P. *Am. J. Clin. Oncol.* **1984**, *7*, 503–505.
(5) Harrap, K. R. *Cancer Treat. Rev.* **1985**, *12* (Supplement A), 21–33.
(6) Rose, W. C.; Schurig, J. E. *Cancer Treat. Rev.* **1985**, *12* (Supplement A), 1–19.
(7) Keppler, B. K.; Schmähl, D. *Arzneim.-Forsch.*, in press.
(8) Clarke, M. J. *Met. Ions Biol. Syst.* **1980**, *11*, 231–276.

0020-1669/87/1326-0844$01.50/0